A Multicore Fiber-Based Velocity Sensor

Xin Ma

***Abstract*—In some special working environments, such as high temperatures, strong electromagnetic fields, dark and narrow spaces, existing technologies such as laser doppler velocimetry (LDV) and high-speed photography velocimetry (HSP) cannot effectively measure the velocity of objects. Multi-core fiber (MCF) is a new type of microstructure optical fiber, which combines the characteristics of traditional optical fibers such as high temperature resistance and electromagnetic field resistance. At the same time, its structure is more compact and its volume is smaller, making it very suitable for working in harsh environments. In this article, we will use the special core layout structure of MCF, combined with their compact volume, to measure the velocity of object. The effects of distance between adjacent fiber cores and the number of cores on average coupling efficiency of spatial light are analyzed. Velocity error caused by the uniformity of fiber core layout is analyzed. An experimental comparison between MCF method and HSP method is conducted to verify the feasibility of the method.**

***Index Terms*—Optical fiber sensing, velocity sensor, multicore fiber (MCF).**

I. Introduction

VELOCITY measurement based on optical methods is widely used in fields such as scientific research, transportation, chemical engineering, energy, and manufacturing. The main measurement methods currently include laser doppler velocimetry, high-speed photography, and other methods. Laser doppler velocimetry (LDV) uses interference fringes to measure object velocity, which has the characteristics of high accuracy and high spatial resolution [1], [2], [3], [4]. However, the light source must be a coherent light source, and the generation of interference fringes requires strict and complicated optical alignment, making the measurement system complex and expensive. High speed photography (HSP) is based on image processing technology, which has a high measurement frequency and can effectively identify subtle changes in objects [5], [6], [7], [8]. However, this technology is mainly limited by factors such as lighting conditions, image exposure, and whether the moving object is well focused. In some special working environments, such as narrow pipelines and strong electromagnetic interference, LDV and HSP cannot perform effective measurements. Multi-core fiber (MCF) is a new type of microstructure fiber that contains multiple cores within the same cladding [9], [10], [11], [12], [13], [14], [15]. Compared to conventional optical fibers, MCF can simultaneously transmit multiple optical signals, serve as both optical sensing and transmission devices, and have a more compact structure and smaller size. In this article, we will use the special core layout structure of MCF, combined with their compact volume, to measure the motion velocity of objects. The research content of this article includes: (1) Analysis of average coupling efficiency of MCF (2) Analysis of velocity error of MCF (3) Experimental research. This work will provide a new method for velocity measurement based on optical methods, which is expected to be applied to harsh conditions such as extremely limited measurement space, strong electromagnetic interference, and high temperature.

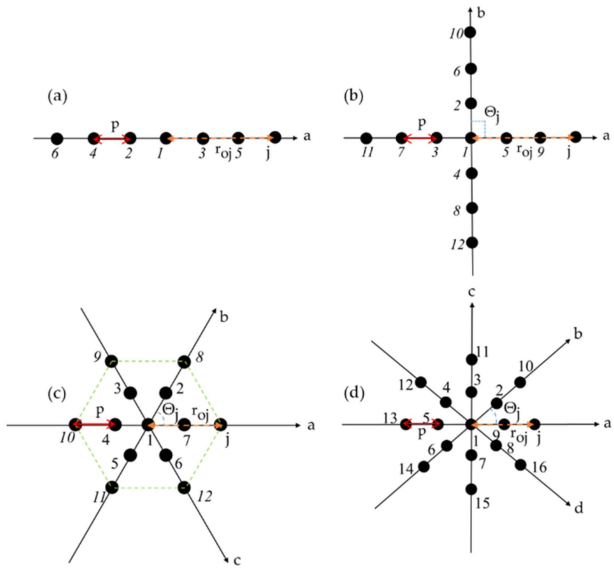

Fig. 1. Four types of MCFs: (a) Single axis distribution structure (b) cross distribution structure (c) regular hexagonal distribution structure (d) double cross distribution structure.

II. Principle

Based on the current reported MCF and the characteristics of fiber core layout [9], [10], [11], [12], [13], [14], [15], we classify MCF into four categories: single axis distribution structure, cross distribution structure, regular hexagonal distribution structure, and double cross distribution structure, as shown in Fig. 1. The first type of structural feature is that the fiber cores are uniformly distributed on a single axis a as shown in Fig. 1(a); the second type of structural feature is that the fiber cores are uniformly distributed on the a and b axes, and the angle between adjacent axes is $\pi/2$ as shown in Fig. 1(b); the third type of structural

Manuscript received 5 December 2023; revised 17 January 2024; accepted 19 January 2024. Date of publication 23 January 2024; date of current version 6 February 2024. This work was supported in part by the National Natural Science Foundation of China under Grant 42361075, in part by the Major Science and Technology Project of Ningxia Autonomous Region under Grant 2022BDE03006, and in part by the Natural Science Foundation of Ningxia Province under Grant 2022AAC03117.

The author is with the Ningxia Key Laboratory of Desert Information & Intelligent Sensing, School of Electronic and Electrical Engineering, Ningxia University, Yinchuan 750021, China (e-mail: maxin_ersa@nxu.edu.cn).

Digital Object Identifier 10.1109/JPHOT.2024.3357548

feature is that the fiber cores are uniformly distributed on the a, b, c axes; and the angle between adjacent two axes is $\pi/3$ as shown in Fig. 1(c); the forth type of structural feature is that the fiber cores are uniformly distributed on the a, b, c, and d axes, and the angle between adjacent two axes is $\pi/4$ as shown in Fig. 1(d). If the fiber core located at the center of the MCF is considered as the origin, there is a positional offset r_{oj} between the origin and the j_{th} fiber core, and the angle between the two adjacent axes is Θ_j.

The measurement method of velocity is based on a principle called spatial filtering velocimetry [16]: Taking Fig. 1(a) as an example, typically, the uniformly arranged fiber cores on a- axis form an array of fiber cores. When an object passes along the a-axis direction at velocity v, the reflected or scattered light of the object will be sequentially received by the fiber cores on the a-axis to generate a periodic signal with a frequency of f_a. The relationship between this signal and the velocity of the object is:

$$v = f_a\ p/m \tag{1}$$

Where m is the magnification of the imaging system.

If an object passes through a multicore fiber with a multi axis structure (cross, hexagon, double cross structure), taking Fig. 1(b) as an example, the velocity v is composed of two velocity components: velocity v_a and velocity v_b:

$$v_a = v\cos\Theta_j,\ \ v_b = v\sin\Theta_j \tag{2}$$

where v_a and v_b can be determined by the following methods:

$$v_a = f_a\ p/m,\ \ v_b = f_b\ p/m \tag{3}$$

where f_a is the frequency of the output signal of the fiber core array on the a-axis, and f_b is the frequency of the output signal of the fiber core array on the b-axis. Other measurement methods for multi axis structures (hexagon, double cross structure) can refer to the above methods.

A. Analysis of Spatial Optical Coupling Efficiency in MCFs.

The coupling between MCF and space light is very important. From the above analysis, it can be seen that the number and layout structure of cores in different types of MCF are different. In this section, we will analyze the impact of these factors on the coupling between MCF and spatial light.

If the fiber core located at the center of the MCF is considered as the origin, there is a positional offset r_{oj} between the origin and the j_{th} fiber core, and the angle between the two adjacent axes is Θ_j, the coupling efficiency of the j_{th} fiber core to spatial light is:

$$\begin{aligned}\eta_j &= \frac{\left|\iint A_L^*(r_{lj})\, B_L(r_{lj}, r_{oj})\, ds\right|^2}{\iint |A_L(r_{lj})|^2 ds \cdot \iint |B_L(r_{lj}, r_{oj})|^2 ds} \\ &= \frac{\left|\int_0^R \sqrt{\frac{8\pi}{\omega_a^2}} \exp\left(-\frac{r_{lj}^2}{\omega_a^2}\right) J_0\left(\frac{2\pi}{\lambda f_0} r_{lj} r_{oj}\right) r_{lj} dr_{lj}\right|^2}{\pi R^2}\end{aligned} \tag{4}$$

Where $A_L(r_{lj})$ is the mode field of the incident light at the distance r_{lj} from the center of the pupil on the incident pupil surface, $A_L^*(r_{lj})$ is its conjugate, and $B_L(r_{lj}, r_{oj})$ is the backward transmission mode field of a single mode fiber located at the incident pupil surface r_{lj}, R is the radius of the coupling lens, ω_a is the backward transmission mode field radius of a single mode fiber, λ is the wavelength, and f_0 is the focal length.

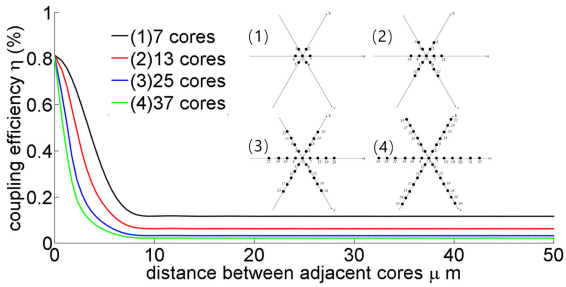

Fig. 2. Effect of distance between adjacent fiber cores on average coupling efficiency η_{av} of hexagon array.

J_0 is a Bessel function:

$$J_0(x) = \frac{1}{2\pi}\int_0^{2\pi} \exp(ix\cos\Theta_j) d\Theta_j \tag{5}$$

Where i is an imaginary number ($i^2 = -1$)

Define a coupling parameter:

$$\beta = \frac{R}{\omega_a} = \frac{\pi R\omega_0}{\lambda f_0} = \frac{\pi D\omega_0}{2\lambda f_0} \tag{6}$$

Where ω_0 is the mode field radius of a single mode fiber.

If $\rho = r_{lj}/R$ is set, then $\eta_j$can be further simplified as

$$\eta_j = \frac{\left|\int_0^1 \sqrt{8\pi}\beta \exp\left(-\beta^2\varrho^2\right) J_0\left(2\beta\frac{r_{oj}}{\omega_0}\varrho\right) \varrho d\varrho\right|^2}{\pi} \tag{7}$$

Average coupling efficiency of n cores in MCF is:

$$\eta_{av} = \frac{\sum_{j=1}^{n} \eta_j}{n} \tag{8}$$

Where n is the total number of cores of MCF.

III. Results and Discussion

According to (8), we calculate and analyze the effect of distance between adjacent fiber cores on the average coupling efficiency of spatial light to multicore fibers, including average coupling efficiency of hexagonal distribution structure MCF, cross distribution structure MCF, and double cross distribution structure MCF.

For the hexagonal distribution of fiber cores, as shown in Fig. 2, the horizontal axis represents the distance between adjacent fiber cores, and the vertical axis represents the average spatial optical coupling efficiency of MCFs. As the distance gradually increases, the average coupling efficiency changes of MCFs represented by 7 cores, 13 cores, 25 cores, and 37 cores are divided into two stages. In the first stage, as the distance increases, the average coupling efficiency of all four types of MCFs continues to decrease. In the second stage, when the distance increases to a certain extent, the average coupling efficiency does not change significantly. When the distance is same, the average coupling efficiency of 7 cores is higher than that of 13 cores, 25 cores, and 37 cores. The smaller the number of fiber cores, the higher the average coupling efficiency.

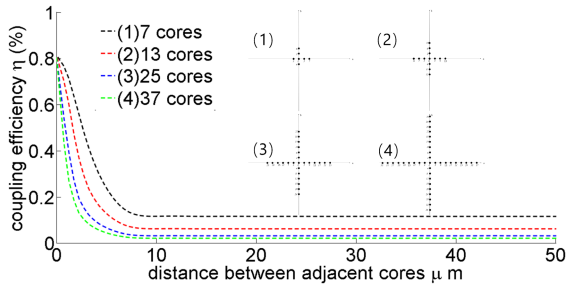

Fig. 3. Effect of distance between adjacent fiber cores on average coupling efficiency η_{av} of cross array.

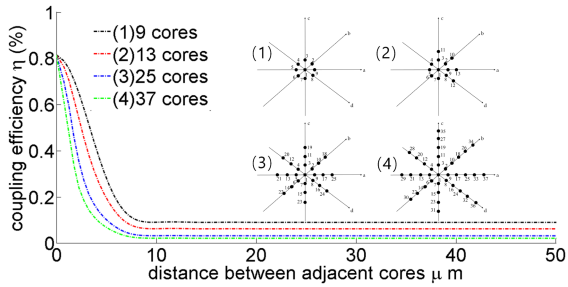

Fig. 4. Effect of distance between adjacent fiber cores on average coupling efficiency η_{av} of the double cross array.

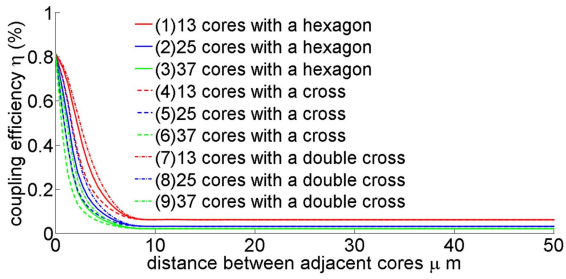

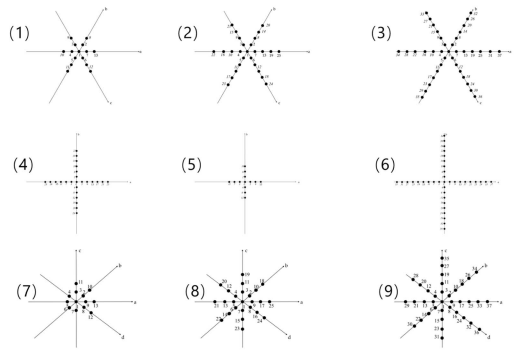

Fig. 5. Comparison of average coupling efficiency η_{av} of three types of MCFs.

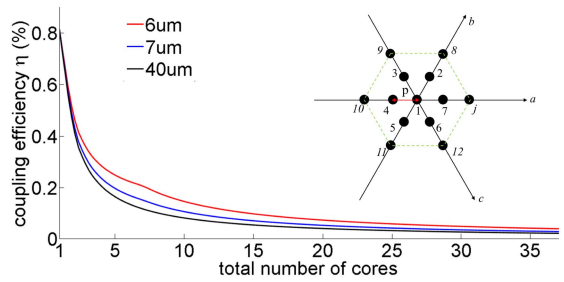

Fig. 6. Effect of the number of cores on average coupling efficiency η_{av} of hexagon array.

For the cross distribution of fiber cores, as shown in Fig. 3, the horizontal axis represents the distance between adjacent fiber cores, and the vertical axis represents the average spatial optical coupling efficiency of MCFs. As the distance gradually increases, the average coupling efficiency changes of MCFs represented by 7 cores, 13 cores, 25 cores, and 37 cores are divided into two stages. In the first stage, as the distance increases, the average coupling efficiency of all four types of MCFs continues to decrease. In the second stage, when the distance increases to a certain extent, the average coupling efficiency does not change significantly. When the distance is same, the coupling efficiency of 7 cores is higher than that of 13 cores, 25 cores, and 37 cores. The smaller the number of fiber cores, the higher the average coupling efficiency.

For the double cross distribution of fiber cores, as shown in Fig. 4, the horizontal axis represents the distance between adjacent fiber cores, and the vertical axis represents the average spatial optical coupling efficiency of MCFs. As the distance gradually increases, the coupling efficiency changes of MCFs represented by 7 cores, 13 cores, 25 cores, and 37 cores are divided into two stages. In the first stage, as the distance increases, the average coupling efficiency of all four types of MCFs continues to decrease. In the second stage, when the distance increases to a certain extent, the average coupling efficiency does not change significantly. When the distance is same, the coupling efficiency of 7 cores is higher than that of 13 cores, 25 cores, and 37 cores. The smaller the number of fiber cores, the higher the average coupling efficiency.

Comparing the average coupling efficiency of three structures as shown in Fig. 5. In the first stage, average coupling efficiency of three structures decreases with the increase of distance between adjacent fiber cores. In the case of the same number of fiber cores, the coupling efficiency of the double cross structure is the highest, followed by the hexagonal structure, and the cross structure is the lowest. In the second stage, average coupling efficiency of three structures does not significantly change with the increase of the distance: In the case of the same number of fiber cores, the coupling efficiency of the three types tends to be the same.

According to (8), we calculate and analyze the effect of the number of fiber cores on the average coupling efficiency of spatial light to MCFs, including the average coupling efficiency of hexagonal distribution structure MCF, cross distribution structure MCF, and double cross distribution structure MCF.

For the hexagonal distribution of fiber cores, as shown in Fig. 6, the horizontal axis represents the number of cores in multi-core optical fibers, and the vertical axis represents the average spatial optical coupling efficiency of MCF. As the number of cores increases, the average coupling efficiency of all MCFs decreases. When the number of fiber cores is the same, the coupling efficiency of MCFs with a distance between adjacent fiber cores of 6 microns is the highest, followed by 7 microns, and 40 microns is the lowest. The average spatial optical coupling

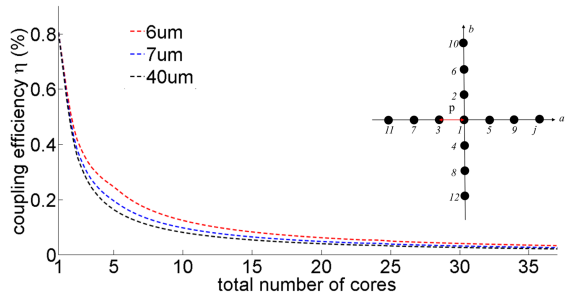

Fig. 7. Effect of the number of cores on average coupling efficiency η_{av} of cross array.

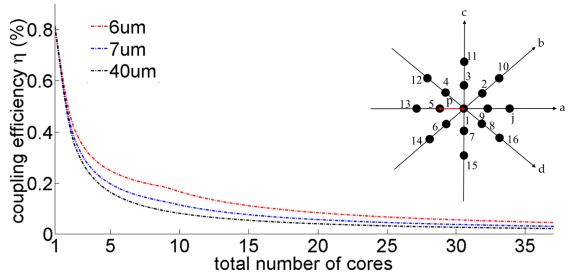

Fig. 8. Effect of the number of cores on average coupling efficiency η_{av} of the double cross array.

efficiency decreases with the increase of the distance between adjacent fiber cores.

For the cross distribution of fiber cores, as shown in Fig. 7. The average coupling efficiency of all MCFs decreases as the number of cores increases. In the case of the same number of fiber cores, the average coupling efficiency of MCFs with a distance between adjacent fiber cores of 6 microns is the highest, followed by 7 microns, and 40 microns is the lowest, which indicates that the average coupling efficiency decreases with the increase of the distance between adjacent fiber cores.

For the double cross distribution of fiber cores, as shown in Fig. 8. As the number of cores increases, the average coupling efficiency of all MCFs decreases. When the number of fiber cores is the same, the coupling efficiency of MCFs with a distance between adjacent fiber cores of 6 microns is the highest, followed by 7 microns, and 40 microns is the lowest. The average coupling efficiency decreases with the increase of the distance between adjacent fiber cores.

As shown in Fig. 9, the average coupling efficiency of three different types decreases with the increase of the number of fiber cores; when the distance between adjacent fiber cores is 6 microns, the coupling efficiency of double cross distribution is the highest, followed by hexagonal distribution, and cross distribution have the lowest coupling efficiency; when the spacing between adjacent fiber cores is 7 microns, the coupling efficiency of double cross distribution is the highest, followed by hexagonal distribution, and cross distribution have the lowest coupling efficiency; When the spacing between adjacent fiber cores is 40 microns, the coupling efficiency of three different types tends to be the same. The difference in average coupling efficiency between three different types will decrease as the fiber core increases.

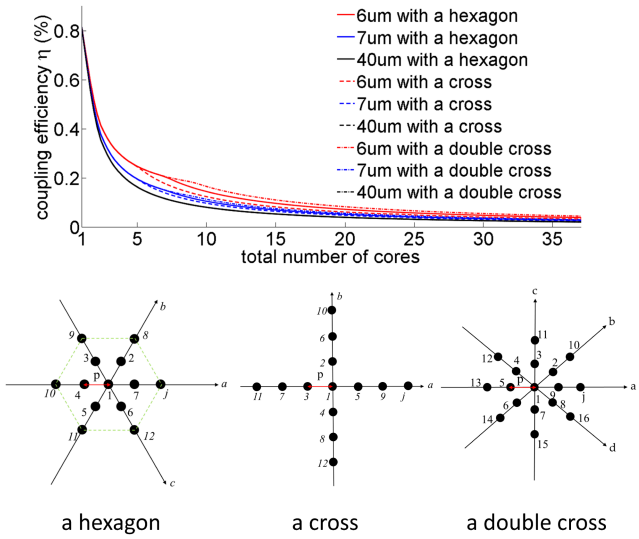

Fig. 9. Comparison of average coupling efficiency η_{av} of different structure MCFs.

From the above comparison, it can be seen that the average coupling efficiency of MCF with the double cross distribution is the highest, followed by the hexagonal distribution, and the cross distribution has the lowest coupling efficiency; The influence of distance between adjacent cores and the number of cores on average coupling efficiency is relatively obvious in the early stage of growth, but the influence on coupling efficiency will gradually slow down after reaching a certain number. A smaller distance between adjacent cores is beneficial for improving average coupling efficiency.

At the same time, in engineering applications, it is also necessary to consider the manufacturing difficulty and cost of MCFs. For example, although the double cross type has the highest average coupling efficiency, the manufacturing process is relatively difficult. In contrast, hexagonal type, although the average coupling efficiency is in the middle, have lower costs, and have been commercially produced. Simply increasing the number of fiber cores not only reduces the average coupling power, but also increases manufacturing difficulties and costs.

A. Analysis of Velocity Error Caused by the Uniformity of Fiber Core Layout

In the early stages of the development of multi-core l fibers, each MCF had only a few cores, such as three cores [9]. With the development of multi-core fiber technology, MCF with more cores were manufactured, such as 36 cores [11], making the manufacturing process more complex and potentially causing uneven distribution between cores. We will analyze the impact of non-uniformly arranged fiber cores on velocity measurement.

For an array composed of n + 1 fiber cores in a certain direction, as shown in Fig. 10, the distances between adjacent fiber cores are $p_1, p_2 \ldots p_n$, respectively.

The difference between two adjacent cores can be expressed as:

$$\Delta p_n = p_n - p_{n-1} \tag{9}$$

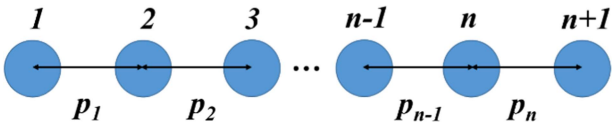

Fig. 10. N segment fiber core array composed of n + 1 fiber cores.

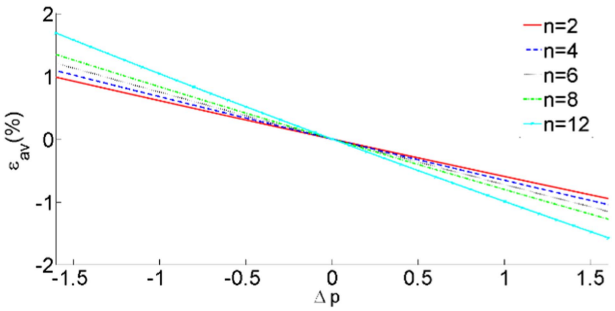

Fig. 11. Impact of core arrangement uniformity on average error ε_{av} of velocity.

In an ideal situation where the fiber cores are evenly arranged, there are $p_1 = p_2 = \ldots = p_n = p$, so $\Delta p_n = 0$.

In the case of non-uniform arrangement of fiber cores, $p_n \neq p_{n-1}$, so $\Delta p_n \neq 0$.

When a moving object passes through adjacent p_{n-1} and p_n with velocity v, according to (1), and assume a relative error:

$$\varepsilon_v = \frac{e_v}{v} = \frac{p}{m}\left(\frac{1}{p_{n-1}+p_n} - \frac{1}{2p}\right) \tag{10}$$

If an object passes through the entire n-segment fiber core array with velocity v, the average velocity error can be expressed as:

$$\varepsilon_{av} = \frac{\sum \varepsilon_v}{n} \tag{11}$$

Refer to the MCF parameters produced by YOFC company ($p = 41.5$ micrometers, $\Delta p_n = \pm 1.6$ micrometers), Fig. 11 describes the uniformity of fiber core layout and the impact of fiber core number on the average velocity error. As the absolute value of Δp_n increases, the absolute value of ε_{av} also increases; as the absolute value of Δp_n decreases, so does the absolute value of ε_{av}. In the case of same Δp_n, the more cores there are, the greater the absolute value of error. From the above analysis, it can be seen that non-uniform arrangement of fiber cores will inevitably affect the measurement of velocity. Therefore, in the actual design and processing of optical fibers, it is necessary to make the fiber cores evenly arranged as much as possible to avoid errors.

B. Experimental Comparison between MCF Method and HSP Method

To verify the feasibility of the presented measurement method, an experimental measurement is conducted. The experiment setup is shown in Fig. 12. The three-core fiber (distance between adjacent cores $p = 41.5$ micrometers, fiber core diameter $r = 8$ micrometers, made by YOFC company) is connected to the circulator and photodetector (PD) through ports 1, 2, and 3

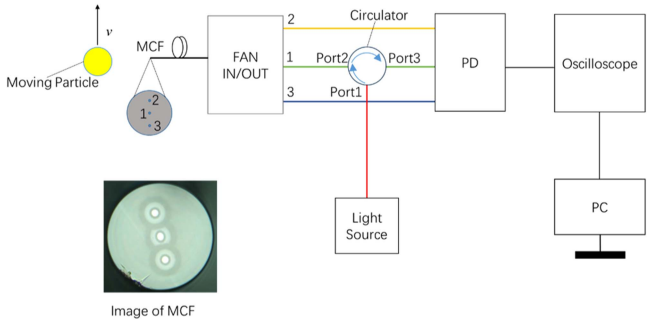

Fig. 12. Experiment setup for velocity measurement.

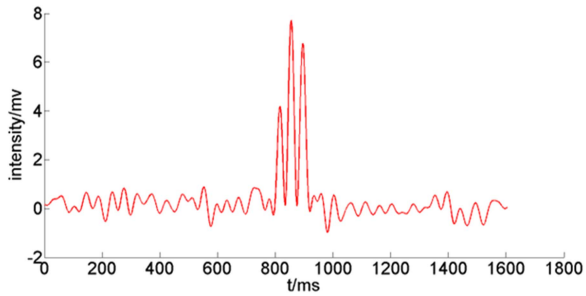

Fig. 13. Example of the measured temporal signal.

of the MCF fan in/out module (FAN IN/OUT). The circulator is connected to the light source -Amplified Spontaneous Emission (ASE) source with a power of 10 mw. The PD is connected to the oscilloscope and PC. The light emitted by the light source passes through ports 1 and 2 of the circulator, and then through port 1 of the MCF FAN IN/OUT module, emitting from core 1 of the three-core fiber. When a particle with a diameter of about 100 microns passes through the end face of the three-core fiber at a velocity v (the velocity of the particle is controlled by a rotator), the light emitted by the three-core fiber will be reflected by the particle and received by the three fiber cores in sequence. The reflected light will enter the PD through the MCF FAN IN/OUT module and the circulator. The PD converts optical signals into electrical signals and sends them to an oscilloscope and PC for analysis. An example of output signal from the PD is shown in Fig. 13. Basically, when the particle passes through the MCF, it will pass through the three cores of the MCF in sequence, and the three cores will receive the reflected light signal of the particle one after another, which means that each fiber core will generate its own temporal signal, finally generating a temporal signal with three peaks.

The maximum value of sensor measurement speed is mainly limited by the bandwidth of photodetector (PD) and the sampling rate of the data collector (oscilloscope). In actual measurement, the bandwidth of PD should be at least equal to the maximum frequency of the velocity signal of the measured object, and the sampling rate of the data collector should be at least 5 times the maximum frequency of the velocity signal of the measured object. The parameters of the above devices directly determine whether the velocity signal of the measured object can be accurately measured. Based on the above principles, combined with the PD parameters (DC-10 MHz) currently used by the

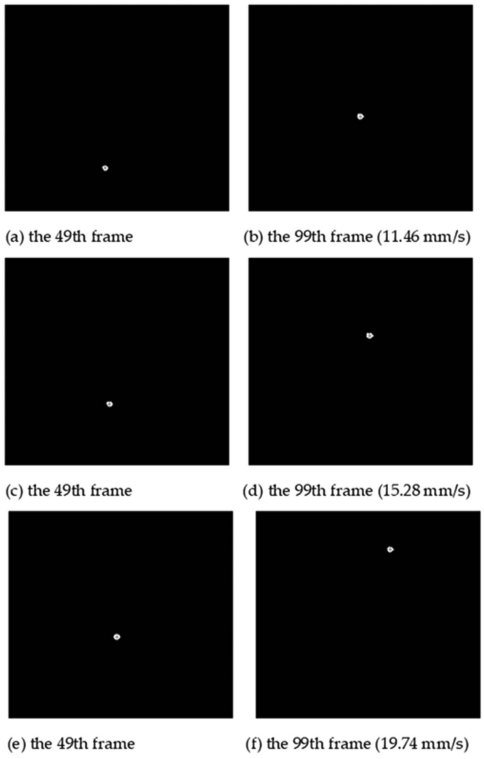

Fig. 14. Binary pictures of the moving particle target with different velocities (captured by phantom high speed camera with 100 frames per second and 719 × 525 pixels, vision research, the USA). Red cross is the center of the particle.

sensor and the oscilloscope parameters (1 GSa/s), the maximum measurable speed of the sensor is 415 m/s theoretically.

HSP is a widely used and valuable technique for measuring object velocity. The basic principle of using HSP can be described as: using high-speed photography to record the motion trajectory of a moving object. The displacement of an object is determined by the change in the position of the object in the two frames of the image, and the velocity is determined by the ratio of displacement to time. To confirm the feasibility of the velocity measurement method proposed in this paper, we conducted HSP experiments for comparison. Fig. 14 shows a set of images of a particle target moving at different speeds captured using HSP. The images in the example have been binarized. In order to obtain the position of the target in the image, it is necessary to first record the pixel coordinates of the target, and then mark the geometric center of the target with a red cross. We can intuitively see from Fig. 14 that for targets moving at the same velocity, the position of the target in the horizontal two frames of the image changes significantly; As the velocity of the target increases from 11.46 mm/s to 19.74 mm/s, the position of the target in the vertical three frame images is also changing, specifically manifested as the faster the velocity, the higher the relative position.

The comparison results between MCF method and HSP method is shown in Fig. 15. The horizontal axis represents the velocity of the object, and the vertical axis represents the measured velocity in Fig. 15. The results show that the MCF method has made some progress in measurement accuracy compared

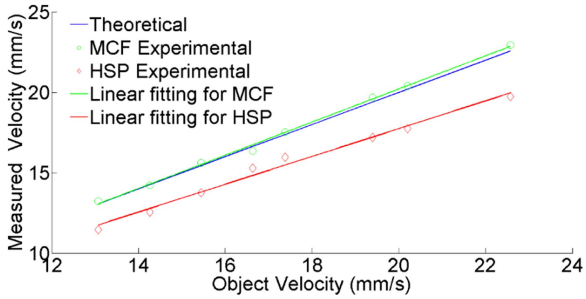

Fig. 15. Comparison results between MCF method and HSP method.

to the HSP method. The reasons that affect the accuracy of HSP may be attributed to factors such as whether the particulate target is well exposed during photography, whether the moving target is well focused, and the accuracy of the HSP system itself. For MCF, due to its end face being close in size to the particle, it can better focus on the observation of small particle movements at closer observation distances and smaller fields of view. Therefore, MCF technology has high measurement accuracy and efficiency in theory. Considering the small and flexible structure of MCF sensing probe, our method may serve as a supplement to HSP in certain fields. For example, for fluid measurement inside centrifugal pumps, a compact probe is easier to place and has less disturbance to the measurement.

The scale of measuring targets mainly depends on the research object and practical applications, rather than the testing limits of optoelectronic devices. Our research object in this article is small-scale particles, and the potential application scenarios of sensors are narrow spaces, strong radiation, and environments with high temperature differences. Therefore, it is necessary to simultaneously consider issues such as particle size, probe size, and the degree of matching between probe and particle size. Our measurement of particles mainly utilizes light scattering. This article is based on the classic Fraunhofer diffraction for the particle. The Fraunhofer diffraction theory is a simplification of Mie scattering theory when the particle size is much larger than the incident light wave (note that the wavelength of the light source used in this article is about 1.5 microns). At present, the size of multi-core optical fibers is generally between 125–300 microns, which is close to the size of particles. This advantage allows the probe to detect particles more accurately. On the other hand, the probe structure is more compact, and the compact probe is easier to arrange. At the same time, it retains the non-contact measurement advantages of optics; Based on the above theoretical analysis and experiments, the measurement range of the object is approximately between 100 and 250 microns. Of course, if it is necessary to detect larger objects, it is possible to consider adding optical lenses, or choose multi-core fibers or fiber arrays that contain more fiber cores.

IV. Conclusion

In this work, we classified existing MCFs, analyzed and compared the effects of distance between adjacent fiber cores and the number cores of MCFs. The results showed that: (1) average coupling efficiency of three structures decreases as the

increase of distance between adjacent fiber cores and the number of fiber cores. (2) average coupling efficiency of MCF with the double cross distribution is the highest, followed by the hexagonal distribution, and the cross distribution has the lowest coupling efficiency. We analyzed velocity error caused by the uniformity of fiber core layout. It showed that: In the case of uneven fiber core layout, the more fiber cores there are, the greater the measurement error.

The above conclusion tells us that in engineering applications, we should choose appropriate types of MCFs for measurement based on specific work conditions. The larger the number of fiber cores and the more complex the structure, the greater the processing error, the higher the cost, and the lower the efficiency.

An experimental comparison between MCF method and HSP method is conducted to verify the feasibility of our method. The results show that the MCF method has made some progress in measurement accuracy compared to the HSP method. Considering the small and flexible structure of MCF sensing probe, our method may serve as a supplement to HSP in certain fields. For instance, for fluid measurement inside centrifugal pumps, a compact probe is easier to place and has less disturbance to the measurement.

REFERENCES

[1] A. O. Ojo et al., "Thermographic laser Doppler velocimetry," *Opt. Lett.*, vol. 40, no. 20, pp. 4759–4762, 2015.

[2] S. Sudo et al., "Analysis of molecular dynamics of colloidal particles in transported dilute samples by self-mixing laser Doppler velocimetry," *Appl. Opt.*, vol. 51, no. 3, pp. 370–377, 2012.

[3] N. Zhou et al., "Investigation of velocity field and oil distribution in an oil-water hydrocyclone using a particle dynamics analyzer," *Chem. Eng. J.*, vol. 157, no. 1, pp. 73–79, 2010.

[4] W. Sun and N. Huang, "Influence of slope gradient on the behavior of saltating sand particles in a wind tunnel," *Catena*, vol. 148, pp. 145–152, 2017.

[5] D. Wang et al., "Statistical analysis of sand grain/bed collision process recorded by high-speed digital camera," *Sedimentology*, vol. 55, no. 2, pp. 461–470, 2008.

[6] Y. Wang et al., "Measurement of sand creep on a flat sand bed using a high-speed digital camera," *Sedimentology*, vol. 56, no. 6, pp. 1705–1712, 2009.

[7] S. Someya et al., "Combined velocity and temperature imaging of gas flow in an engine cylinder," *Opt. Lett.*, vol. 37, no. 23, pp. 4964–4966, 2012.

[8] L. Duarte-Campos et al., "Laser particle counter validation for aeolian sand transport measurements using a high speed camera," *Aeolian Res.*, vol. 25, pp. 37–44, 2017.

[9] R. Ryf et al., "Space-division multiplexed transmission over 4200-km 3-core microstructured fiber," in *Proc. Opt. Fiber Commun. Conf.*, 2012, Paper PDP5C.2.

[10] M. Jinno, T. Kodama, and T. Ishikawa, "Five-core 1×6 core selective switch and its application to spatial channel networking," in *Proc. Opt. Fiber Commun. Conf. Exhib.*, 2020, pp. 1–3.

[11] J. Sakaguchi et al., "Realizing a 36-core, 3-mode fiber with 108 spatial channels," in *Proc. Opt. Fiber Commun. Conf. Exhib.*, 2015, pp. 1–3.

[12] T. Hayashi et al., "End-to-end multi-core fibre transmission link enabled by silicon photonics transceiver with grating coupler array," in *Proc. Eur. Conf. Opt. Commun.*, 2017, pp. 1–3.

[13] D. Soma et al., "2.05 Peta-bit/s super-nyquist-WDM SDM transmission using 9.8-km 6-mode 19-core fiber in full C band," in *Proc. Eur. Conf. Opt. Commun.*, 2015, pp. 1–3.

[14] B. J. Puttnam et al., "2.15 Pb/s transmission using a 22 core homogeneous single-mode multi-core fiber and wideband optical comb," in *Proc. Eur. Conf. Opt. Commun.*, 2015, pp. 1–3.

[15] K. Takenaga et al., "High-density multicore fibers," in *Proc. Opt. Fiber Commun. Conf. Exhib.*, 2016, pp. 1–3.

[16] Y. Aizu and T. Asakura, *Spatial Filtering Velocimetry, Fundamentals*. Berlin, Germany: Springer, 2006.